



Vapor Pressure and Physicochemical Properties of {LiBr + IL-Based Additive + Water} Mixtures: Experimental Data and COSMO-RS Predictions

Marta Królikowska^{1,2} · Michał Skonieczny¹ · Kamil Paduszyński¹ · Maciej Zawadzki¹

Received: 24 June 2020 / Accepted: 11 March 2021 / Published online: 7 April 2021
© The Author(s) 2021

Abstract

In recent years, many compounds have been proposed as additives to conventional working fluids to improve the performance of the absorption refrigeration system. The main aim of this research is to show the influence of ionic liquid based additives on thermodynamic and physicochemical properties of {LiBr+water} solutions. The following additives: 3-(1-methyl-morpholinium)propane-1-sulfonate, *N,N*-di(2-hydroxyethyl)-*N,N*-dimethylammonium bromide, and *N,N,N*-tri(2-hydroxy-ethyl)-*N*-methylammonium bromide have been added to aqueous lithium bromide solutions (IL to LiBr mass fraction, $w_2 = 0.3$). The physicochemical and thermodynamic properties of {LiBr (1)+additive (2)+water (3)} and {LiBr+water} systems including (vapor+liquid) phase equilibria (VLE), density (ρ) and dynamic viscosity (η) were determined over wide temperature and composition ranges. The conductor-like screening model for real solvents (COSMO-RS) was used for the VLE data prediction. For the density and dynamic viscosity correlations, empirical equations were applied. A comparison of experimental data for {LiBr+additive+water} with those for {LiBr+water} systems shows the influence of using the additives proposed in this work. The data presented are complementary to the current state of knowledge in this area and provide directions for future research.

Keywords Additive · {LiBr+water} system · VLE · Density · Viscosity · COSMO-RS

1 Introduction

Concerns about the impact of human related activities and its impact on the environment, as evident in climate change, have altered human behavior in a need to protect the natural environment and save energy and resources. Following this trend, interest in absorption cooling devices as a “greener” alternative to compressor devices has increased significantly in recent

✉ Marta Królikowska
mlaskowska@ch.pw.edu.pl

¹ Physical Chemistry Department, Faculty of Chemistry, Warsaw University of Technology, Noakowskiego 3, 00-664 Warsaw, Poland

² Thermodynamics Research Unit, School of Engineering, University of KwaZulu-Natal, Howard College Campus, King George V Avenue, Durban 4041, South Africa

years. Cold production in these devices is realized by the thermal compressor which uses environmentally friendly refrigerants. Additionally, this technology can operate without the need of (large quantities) electricity since waste or surplus heat is used as an energy source. For these reasons absorption cooling is mostly used in industry where cheap surplus heat is abundant.

The effectiveness of absorption coolers is determined by the properties of the working fluids. Two types of industrial wide-scale absorption refrigerators are in use: lithium bromide + water, or water + ammonia [1]. Corrosion and crystallization as well as explosiveness and toxicity [2–4] are key factors requiring improvement to guarantee safe and stable operation. The search for new working pairs with more favorable properties has gained importance and is being investigated by research groups around the world [5–10].

The easier fix, however, is to improve existing working pairs since this will not require the redesigning of the existing apparatus. In the case of the {LiBr + water} system, the crystallization temperature seems to be one of the main issues.

It has been shown that the presence of a small amount of non-volatile and hygroscopic additive is one method in lowering the crystallization temperature of working fluids. The increase in possible lithium bromide concentration will result in a significant reduction of water vapor pressure, which is desired from the viewpoint of the efficiency of the refrigeration process. Numerous organic compounds are proposed as additives that reduce the crystallinity {LiBr + water} [11–28] but to date only a few publications [29–34] consider the use of ionic liquids (ILs) as additives.

Our work carried out so far in this area concerns a comprehensive study of the solubility of lithium bromide in water in the presence of a total of 33 additives [24, 25, 33, 34], mainly ionic liquids [33, 34], but also zwitterions [25, 34], glycols and crown ethers [24]. The focus of the investigations was to determine the effect of the amount of additive and the structure of the ionic liquid, including the length of the alkyl chain in the cation of the ionic liquid, the functionalization of the substituent in the IL's cation, as well as the structure of the cation core, on solubility in the studied system. In previous papers regarding the crystallization of the LiBr + water mixtures in the presence of an IL or ZI additive, we identified that the greatest increase in solubility of LiBr in water was observed when [MOR_{1,3}SO₃] was added. Additionally, the presence of a hydroxyl group on the ionic liquid cation increases the solubility in the tested system. The second best results were obtained when the ionic liquid [N_{1,1,2OH,2OH}]Br was used as an additive [34].

On the basis of our previous work we have selected [MOR_{1,3}SO₃] and [N_{1,1,2OH,2OH}]Br for further research. Since the addition of hydroxyl groups enhances the solubility we have also selected [N_{1,2OH,2OH,2OH}]Br to be tested as an additive. In this work the (vapor + liquid) phase equilibria (VLE), density and dynamic viscosity of {LiBr + additive + water} are presented. The experimental results are compared to those for the {LiBr + water} system, commercially used in absorption refrigeration technology. The thermodynamic modelling of the investigated systems was performed using the conductor-like screening model for real solvents (COSMO-RS). This approach was selected as it does not require any experimental input, needed in parameterization of other types of models like the mentioned activity coefficients equations and classical or molecular-based equations of state.

2 Experimental Section

2.1 Chemicals Used

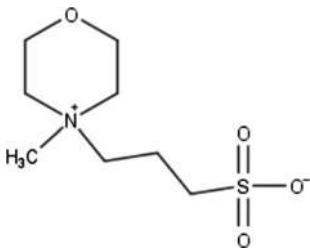
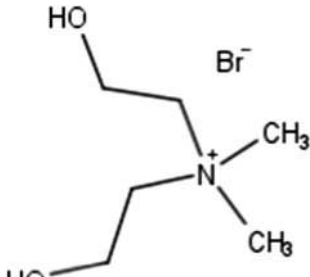
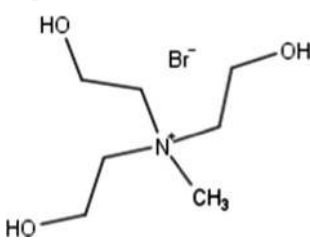
Lithium bromide (CAS No. 7550-35-8) was purchased from Fluka with nominal mass fraction purity > 0.99.

The water was purified using reverse osmosis unit with an ion-exchange system to a conductivity < 0.05 $\mu\text{S}\cdot\text{cm}^{-1}$ (Cobrabid-Aqua, Poland) and next degassed in an ELMA Germany ultrasonic bath at $T=320$ K for half an hour before each measurement.

The structure and basic information of the tested salts are collected in Table 1.

Each IL-based additive was synthesized in our laboratory. A detail description of synthesis procedure of $[\text{N}_{1,2\text{OH},2\text{OH},2\text{OH}}]\text{Br}$ is given below. The structure of the synthesized compounds was confirmed by ^1H NMR and ^{13}C NMR analyses performed with Spectrometer Varian NMR System 500 MHz and Spectrometer Varian Gemini 2000, respectively. Figures S1 and S2 in the supplementary material (SM) present the results of these analyses. The purity estimated from ^1H NMR is higher than 97% wt.

Table 1 The structures of the IL-based additives tested in this work

Structure	Name, abbreviation, CAS No.
	3-(1-methylmorpholinium)propane-1-sulfonate, $[\text{MOR}_{1,3}\text{SO}_3]$; CAS No. 111282-24-7
	<i>N,N</i> -di(2-hydroxyethyl)- <i>N,N</i> -dimethylammonium bromide, $[\text{N}_{1,1,2\text{OH},2\text{OH}}]\text{Br}$; CAS No. 28508-23-8
	<i>N,N</i> -tri(2-hydroxyethyl)- <i>N</i> -methylammonium bromide, $[\text{N}_{1,2\text{OH},2\text{OH},2\text{OH}}]\text{Br}$; CAS No. 38005-22-0

Detailed descriptions of synthesis procedures and thermophysical characterization for $[\text{MOR}_{1,3}\text{SO}_3]$ and $[\text{N}_{1,1,2\text{OH},2\text{OH}}]\text{Br}$ are reported in the previous study [34].

2.1.1 The Synthesis Procedure of *N,N,N*-tri(2-hydroxyethyl)-*N*-methylammonium Bromide, $[\text{N}_{1,2\text{OH},2\text{OH},2\text{OH}}]\text{Br}$

Preparation of *N,N,N*-tri(2-hydroxyethyl)-*N*-methylammonium bromide, $[\text{N}_{1,2\text{OH},2\text{OH},2\text{OH}}]\text{Br}$ was carried out accordingly to a previous reported procedure [35]. To a 500 cm³ flask 49.041 g of methyl diethanolamine (Sigma–Aldrich >98%, 0.4116 mol) dissolved in a 200 cm³ of acetonitrile (POCh for HPLC) was added. Subsequently, 59.949 g of 2-bromoethanol (Sigma–Aldrich 95%, 0.4797 mol, 1.16 eq) was added dropwise into the flask. The mixture was stirred in an oil bath at the temperature $T=353.15$ K for 24 h. During this time two liquid phases were formed. The mixture was cooled to room temperature and the phases were separated. To the heavier phase, 100 cm³ of 2-propanol was added and the mixture was cooled in dry ice. During the slow reheating to the room temperature *N,N,N*-tri(2-hydroxyethyl)-*N*-methylammonium bromide crystallized. The crystals were filtered and washed with 50 cm³ of ethyl acetate and dried at $T=303.15$ K under vacuum to remove the solvents. 81.650 g of white crystalline solid was obtained. Reaction yield was 81.3%.

¹H NMR: δ_{H} (500 MHz; D₂O) ppm: 3.175 (3H, s), 3.58–3.63 (6H, t, $J^3_{\text{H-H}}=5.1$ Hz), 3.96–4.02 (6H, m).

¹³C NMR δ_{C} (200 MHz; D₂O) ppm: 21.494, 26.614, 35.804.

To remove traces of water and volatile compounds each ionic liquid was dried in a vacuum drying oven (Binder, model VD 23) under reduced pressure ($P=0.5$ kPa) obtained by a vacuum pump (Vacuubrand RZ 6) at temperature $T=338.15$ K for at least 72 h before the measurements. Afterwards, the water content was checked by coulometric titration (Karl Fischer method) using KF Trace Titroline (Metrohm, 716 DMS Titrimo). The estimated purity of the chemicals used in this work is presented in Table 2.

2.2 Apparatus and Procedure

2.2.1 Sample Preparation

A solution of lithium bromide was prepared from anhydrous lithium bromide and deionized water by weighing components on a Mettler Toledo XA105 balance with an uncertainty of 0.0001 g. A measured quantity of additive was added to anhydrous lithium bromide such that the (additive to lithium bromide) mass fraction $w_2=0.3$ was obtained. After that, water was added to make the system liquid at room temperature. Then, by adding the appropriate amount of water, a series of ternary {LiBr + additive + water} solutions with well defined compositions ($x_{1+2}=x_1+x_2$, where indices 1 and 2 refer to LiBr and the additive, respectively) were prepared and tested.

2.2.2 (Vapor + Liquid) Phase Equilibria

The VLE data for aqueous lithium bromide solution and {LiBr (1) + additive (2) + water (3)} systems have been measured using an ebulliometric method over a wide composition range at temperatures from 338.15 to 368.15 K with an increment of 10 K at pressures up to $P=85$ kPa. A detailed description of the apparatus was presented in an earlier

Table 2 Specifications of chemical samples^a

Sample	Source	Initial mass fraction purity	Purification method	Final mass fraction purity (wt%) ^a	Analysis method	Water content/ppm
[MOR _{1,3} SO ₃]	Own synthesis	–	Crystallization, vacuum heating	97.0	Karl-Fischer, ¹ H NMR	580
[N _{1,1,2} OH ₂ OH] Br	Own synthesis	–	Crystallization, vacuum heating	97.0	Karl-Fischer, ¹ H NMR	620
[N _{1,2} OH ₂ OH] 2OH] Br	Own synthesis	–	Crystallization, vacuum heating	97.0	Karl-Fischer, ¹ H NMR	650
Water	Own source	–	Reversed osmosis, ion exchange	99.99	density	–
LiBr	Fluka	99.0	–	99.0	–	–
1-Butanol	Sigma–Aldrich	99.8	–	99.8	–	70
Cyclohexane	Sigma–Aldrich	99.5	–	99.5	–	110
2-Propanol	Sigma–Aldrich	99.5	–	99.5	–	150
Octane	Sigma–Aldrich	99.0	–	99.0	–	70

^aThe studied organic salts were isolated as crystals. With only residual volatile solvents from synthesis as impurities. Generally, the actual purity of the salt is higher than > 97% mol. It is accepted that when in ¹H NMR there are no other peaks purity is higher than 97%. The precise values of purity of organic salts were not determined

publication [36]. The equilibrium temperature was measured with a resistance thermometer (type P-550, ROTH, Germany) with the precision of 0.01 K. The pressure was measured with the precision of 0.1 kPa by a tensiometric vacuum meter (type CL 300, ZEPWN, Poland). The thermometer and the manometer were calibrated by measuring the boiling points as a function of pressure for 1-butanol, cyclohexane, octane and water. Due to the extremely low volatility of lithium bromide and IL-base additives, the gas phase is assumed to only consist of water in the tested systems. After an equilibrium state is established, the composition of the liquid phase (x_{1+2}) was determined using the Anton Paar GmbH 4500 vibrating-tube densimeter (Graz, Austria) with an accuracy of $1 \times 10^{-5} \text{ g}\cdot\text{cm}^{-3}$ at each temperature. A calibration curve of density vs. composition (x_{1+2}) was made. The mole fraction composition determination had a standard deviation of $u(x) = 2 \times 10^{-3}$. Every sample was measured in triplicate. From VLE measurements, the vapor pressure as a function composition (x_{1+2}) in the liquid phase is reported at a constant temperature. The uncertainty of the method used for the VLE estimation is larger than the error of the instruments and was estimated from the calibration data $u(P) = 0.5 \text{ kPa}$.

2.2.3 Density Measurements

The liquid density data of {LiBr (1) + water (2)} and {LiBr (1) + additive (2) + water (3)} was determined at $P = 0.1 \text{ MPa}$ using the Anton Paar GmbH 4500 vibrating-tube densimeter (Graz, Austria). The apparatus has an automatic correction for the viscosity of the sample. The uncertainty of the measurements was estimated to be better than $5 \times 10^{-4} \text{ g}\cdot\text{cm}^{-3}$. Two integrated Pt 100 platinum thermometers, calibrated by the producer, provided good precision in temperature control (internally of 0.01 K). The density of the tested mixtures was determined over the temperature range from 298.15 to 343.15 K with an increment of 5 K over a wide composition range.

2.2.4 Dynamic Viscosity Measurements

The experiment was performed using an Anton Paar GmbH AMVn (Graz, Austria) programmable viscometer, with a nominal uncertainty of 5% for viscosities from (0.3 to 2500) mPa·s. Before the experiment, the apparatus was calibrated using the standard provided by the supplier. During the experiment, the temperature was controlled internally to a precision of 0.01 K in a range from 298.15 to 348.15 K with an increment of 5 K. Over the measured viscosity range, capillaries of varying diameters were used depending on the viscosities of the fluid. The diameter of the capillary was 1.6 mm (ball diameter 1.5 mm) for viscosity in the range from 0.3 to 10 mPa·s, 1.8 mm (ball diameter 1.5 mm) for viscosity in range from 2.5 to 70 mPa·s and 3.0 mm (ball diameter 2.5 mm) for viscosity in the range from 20 to 230 mPa·s.

3 COSMO-RS Prediction

To gain insights into the mixture behavior, a molecular based thermodynamic approach can be applied. For the purpose of this study, the most suitable tool was the conductor-like screening model for real solvents (COSMO-RS) proposed and developed by Klamt and Eckert [37]. In comparison with commonly used excess Gibbs energy models, like Wilson's equation, NRTL or UNIQUAC, this model is very versatile as it allows to predict

liquid phase activity coefficients, hence the related thermodynamic properties of fluids as well. If the modelling of these mixtures were successful, then this model could be applied in computer-aided molecular design of new IL-based additives for the {LiBr + water} system. All the details on the model, including its foundations and derivations, can be found elsewhere [38]. Herein, we provide only a brief summary and computational details on its implementation.

The only information required by COSMO-RS to get the chemical potential, thus phase equilibria, is the chemical structure of the molecules forming the system. Based on the molecular geometries fully optimized by using quantum chemical methods, the screening charge distribution (σ) at the surface of molecular cavities in a perfect conductor is obtained for each moiety; this is the COSMO part of the model. The spatial distribution is then converted to a histogram of specific charge density values, called the σ -profile. Then, the ensemble of charged segments according to the σ -profiles is considered and treated by using the methods of statistical thermodynamics, to finally get the formulas for the chemical potential of segment and molecular component; this is the “COSMO-RS” part of the model. In this work, the COSMO $therm$ suite [39] purchased from BIOVIA/3DS was utilized to obtain the computed results. Molecular geometries/conformations of all the molecules and the corresponding COSMO-files were generated by using TURBOMOLE [40] and COSMO $conf$ utilities provided by the BIOVIA/3DS as well. All the files are readily available upon e-mail request. The level of calculations performed to get the σ -profiles was BP-TZVP-COSMO, i.e. Becke–Pedrew (BP) functional for DFT calculations [41, 42] combined with triple- ζ functional basis set [43] and “conventional” COSMO solvation method [44] for molecular cavity. The COSMO-RS parametrization employed was BP_TZVP_18.

In this work, the calculations were performed using standard setup of the software (COSMO $conf$ /TURBOMOLE for geometry optimization and the COSMO $therm$ for thermodynamic calculations) and the parameterization used. Individual σ -profiles (thus, the COSMO-files) for each actual moiety found in the mixtures under study were adopted: water, Li⁺ cation, Br⁻ anion, IL cation.

4 Results and Discussion

4.1 (Vapor + Liquid) Phase Equilibria, VLE Measurements

The accurate (vapor+liquid) phase equilibrium data for an aqueous lithium bromide solution is necessary for developing and extending the performance range of absorption refrigeration machines. In this work, the VLE data of aqueous lithium bromide solutions was determined using the isothermal ebulliometric method at temperatures from 338.15 to 368.15 K for a wide range of lithium bromide concentrations. The experimental data, including vapor pressure versus LiBr mole fraction at different temperatures, are collected in Table 3 and graphically presented in Fig. 1.

In the open literature vapor pressure–temperature–composition diagrams for {LiBr + water} systems have been presented many times [45–53]. A number of methods for measuring the vapor pressure of aqueous lithium bromide solutions including: static, ebulliometric, gas transport, differential static, or bubble point methods were used. Pátek and Klomfar [54] presented an effective formulation of the thermodynamic properties of aqueous lithium bromide solutions up to 500 K over the whole concentration range. They have also shown a short comparison of literature data from different experimental

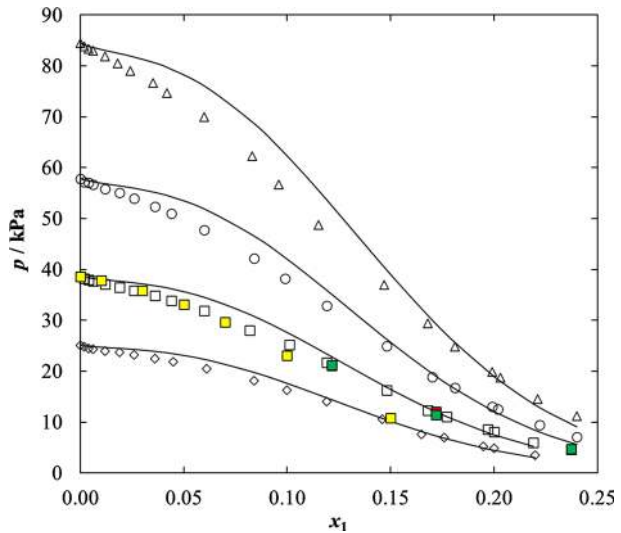
Table 3 Isothermal experimental P – T – x data for the {LiBr (1) + water (2)} binary system: T , equilibrium temperature; P , equilibrium pressure; x_1 , lithium bromide mole fraction; γ_2 , activity coefficient of water calculated based on the experimental data

x_1	P (kPa)	γ_2	x_1	P (kPa)	γ_2
$T = 338.15$ K					
0.000	25.1	1.000	0.084	18.1	0.787
0.002	24.8	0.990	0.100	16.3	0.722
0.004	24.5	0.980	0.119	14.0	0.633
0.006	24.3	0.974	0.146	10.5	0.490
0.012	24.0	0.968	0.165	7.56	0.361
0.019	23.7	0.963	0.176	6.92	0.335
0.026	23.2	0.949	0.195	5.18	0.256
0.036	22.5	0.930	0.200	4.82	0.240
0.045	21.8	0.909	0.220	3.54	0.181
0.061	20.5	0.870			
$T = 348.15$ K					
0.000	38.6	1.000	0.082	28.1	0.793
0.002	38.2	0.992	0.101	25.2	0.726
0.004	37.9	0.986	0.119	21.7	0.638
0.006	37.7	0.983	0.148	16.3	0.496
0.012	37.1	0.973	0.168	12.3	0.383
0.019	36.5	0.964	0.177	11.0	0.346
0.026	35.9	0.955	0.197	8.57	0.276
0.036	34.8	0.935	0.200	8.02	0.260
0.044	33.9	0.919	0.219	6.01	0.199
0.060	31.9	0.879			
$T = 358.15$ K					
0.000	57.8	1.000	0.084	42.2	0.797
0.002	57.2	0.992	0.099	38.2	0.734
0.004	57.0	0.990	0.119	32.9	0.646
0.006	56.7	0.987	0.148	24.9	0.506
0.012	55.8	0.977	0.170	18.9	0.394
0.019	55.1	0.972	0.181	16.7	0.353
0.026	53.9	0.957	0.199	13.1	0.283
0.036	52.4	0.940	0.202	12.5	0.271
0.044	51.0	0.923	0.222	9.39	0.209
0.060	47.7	0.878	0.240	7.10	0.162
$T = 368.15$ K					
0.000	84.4	1.000	0.083	62.3	0.805
0.002	83.8	0.995	0.096	56.7	0.742
0.004	83.3	0.991	0.115	48.7	0.652
0.006	83.0	0.989	0.147	36.9	0.513
0.012	81.9	0.982	0.168	29.4	0.419
0.018	80.5	0.971	0.181	24.8	0.359
0.024	79.1	0.960	0.199	19.9	0.294
0.035	76.6	0.940	0.203	18.8	0.279
0.042	74.7	0.923	0.221	14.5	0.221
0.060	70.0	0.882	0.240	11.2	0.175

Table 3 (continued)

Standard uncertainties u are as follows: $u(x_1)=2 \times 10^{-3}$; $u(P)=0.5$ kPa, $u(T)=0.05$ K

Fig. 1 Isothermal experimental P - T - x data for the {LiBr (1)+ water (2)} binary system at different temperatures: open diamond, 338.15 K; open square, 348.15 K; open circle, 358.15 K; open triangle, 368.15 K. Points—experimental data; solid lines, COSMO RS predictions. Literature VLE data at $T=348.15$ K: filled green square, Ref. [47]; filled red square, Ref. [48]; filled yellow square, Ref. [49] (Color figure online)



techniques, giving also the range of temperature, pressure and composition in each case. As is shown in Fig. 1, the experimental results presented in this work are in good agreement with the literature data. The experimental data presented in this work show the highest deviations (RMSD = 1.86 kPa) compared to the data presented by Sada et al. [49]. The best agreement (RMSD = 0.37 kPa) was shown with the data published by Boryta et al. [48].

In order to know how the additive influenced the vapor pressure of aqueous lithium bromide solution, the VLE measurements for {LiBr (1) + [MOR_{1,3}SO₃], or [N_{1,1,2OH,2OH}]Br, or [N_{1,2OH,2OH,2OH}]Br (2) + water (3)} ternary systems were performed. The experimental data were measured at temperatures between 338.16 and 368.15 K with an increment of 10 K, at compositions up to $x_{1+2}=0.35$. Tables 4, 5, and 6 include all experimental VLE results and the calculated value of the activity coefficients of water in the tested systems. Figure 2 presents the VLE data for {LiBr (1) + [MOR_{1,3}SO₃] (2) + water (3)}, as an example. The data for the other systems tested in this work are presented graphically in Figs. S3 and S4 (supplementary material). In the figures, x_{1+2} was defined as $x_1 + x_2$ at the equilibrium state. The tabulated data of compositions for lithium bromide and additive mole fractions at the equilibrium state are also presented in Tables 4, 5 and 6. In each case, vapor pressures increase with temperature but decrease with an increase in the composition (x_{1+2}).

The comparison of the VLE data for all tested binary and ternary systems is presented in Fig. 3. It can be noticed that the addition of each tested compound causes an increase in vapor pressure, which is not desirable for the process taking place in the absorber. On the other hand, increasing the vapor pressure of the system is favorable for the process taking place in the generator. The process of evaporating the refrigerant (water) from the ternary system is then facilitated, which is associated with lower energy consumption. The highest effect is observed when [MOR_{1,3}SO₃] was added to the aqueous lithium bromide solution. The activity coefficients of water (γ_3) were calculated in each of the tested systems. The

Table 4 Experimental and calculated P - x data for the systems {LiBr (1)+[MOR_{1,3}SO₃] (2)+ water (3)}, $w_2=0.3003$ at different temperatures from 338.15 to 368.15 K; w_2 , (additive to LiBr) mass fraction; x_1 , lithium bromide mole fraction at the equilibrium state; x_2 , additive mole fraction at the equilibrium state; P , equilibrium pressure; T , equilibrium temperature; γ_3 , activity coefficient of water calculated based on the experimental data

x_1	x_2	P (kPa)	γ_3	x_1	x_2	P (kPa)	γ_3
T=338.15 K							
0.0000	0.0000	25.1	1.000	0.0764	0.0127	19.2	0.840
0.0029	0.0005	24.6	0.983	0.0896	0.0149	17.6	0.783
0.0069	0.0012	24.3	0.976	0.1038	0.0173	15.9	0.721
0.0121	0.0020	24.1	0.974	0.1235	0.0206	13.5	0.628
0.0188	0.0031	23.7	0.965	0.1387	0.0231	11.9	0.566
0.0282	0.0047	23.1	0.952	0.1647	0.0275	9.11	0.449
0.0422	0.0070	22.2	0.930	0.1844	0.0307	7.01	0.356
0.0582	0.0097	20.9	0.893				
T=348.15 K							
0.0000	0.0000	38.6	1.000	0.0767	0.0128	29.3	0.833
0.0029	0.0005	37.9	0.985	0.0894	0.0149	27.2	0.786
0.0069	0.0011	37.6	0.982	0.1044	0.0174	24.6	0.726
0.0122	0.0020	37.3	0.980	0.1265	0.0211	20.7	0.629
0.0183	0.0030	36.7	0.971	0.1413	0.0236	18.4	0.571
0.0284	0.0047	35.7	0.956	0.1628	0.0271	14.4	0.461
0.0434	0.0072	34.2	0.934	0.1858	0.0310	11.2	0.371
0.0575	0.0096	32.3	0.897	0.2195	0.0366	6.19	0.216
T=358.15 K							
0.0000	0.0000	57.8	1.000	0.0770	0.0128	44.1	0.838
0.0029	0.0005	57.0	0.989	0.0895	0.0149	40.8	0.788
0.0068	0.0011	56.6	0.987	0.1053	0.0175	37.2	0.734
0.0124	0.0021	56.0	0.983	0.1237	0.0206	31.7	0.641
0.0186	0.0031	55.2	0.977	0.1403	0.0234	28.0	0.579
0.0281	0.0047	53.8	0.963	0.1655	0.0276	21.5	0.461
0.0432	0.0072	51.4	0.936	0.1843	0.0307	17.3	0.381
0.0575	0.0096	48.4	0.898	0.2182	0.0364	9.94	0.231
T=368.15 K							
0.0000	0.0000	84.4	1.000	0.0765	0.0128	65.2	0.848
0.0029	0.0005	83.5	0.992	0.0932	0.0155	59.6	0.793
0.0069	0.0012	82.7	0.988	0.1059	0.0177	54.7	0.740
0.0123	0.0020	81.9	0.984	0.1253	0.0209	46.9	0.651
0.0181	0.0030	80.6	0.975	0.1396	0.0233	41.6	0.589
0.0283	0.0047	78.8	0.966	0.1634	0.0272	32.3	0.473
0.0424	0.0071	75.0	0.934	0.1855	0.0309	25.8	0.390
0.0572	0.0095	70.8	0.899	0.2285	0.0381	15.6	0.252

$$w_2 = \frac{m_2}{m_1+m_2}$$

Standard uncertainties u are as follows: $u(x_1)=2 \times 10^{-3}$; $u(P)=0.5$ kPa, $u(T)=0.05$ K

calculated values are below unity, which indicates the occurrence of negative deviations compared to an ideal system.

The addition of the tested compounds into the {LiBr (1)+water (2)} system causes a slight increase in the value of the coefficients. As shown in Fig. 3, the activity coefficient of water in the tested systems, γ_3 , increases in the following order: [N_{1,1,2OH,2OH}]

Table 5 Experimental and calculated $P-x$ data for the systems {LiBr (1) + [N_{1,1,2OH,2OH}] Br (2) + water (3)}, $w_2 = 0.2996$ at different temperatures from 338.15 to 368.15 K; w_2 , (additive to LiBr) mass fraction; x_1 , lithium bromide mole fraction at the equilibrium state; x_2 , additive mole fraction at the equilibrium state; P , equilibrium pressure; T , equilibrium temperature; γ_3 , activity coefficient of water calculated based on the experimental data

x_1	x_2	P (kPa)	γ_3	x_1	x_2	P (kPa)	γ_3
T = 338.15 K							
0.0000	0.0000	25.1	1.000	0.0767	0.0133	18.4	0.806
0.0043	0.0007	24.4	0.977	0.0836	0.0145	17.1	0.755
0.0094	0.0016	24.1	0.971	0.1174	0.0204	11.2	0.518
0.0153	0.0027	23.8	0.966	0.1386	0.0240	9.57	0.456
0.0231	0.0040	23.3	0.954	0.1655	0.0287	7.38	0.365
0.0353	0.0061	22.3	0.926	0.1868	0.0324	4.91	0.250
0.0560	0.0097	20.6	0.879				
T = 348.15 K							
0.0000	0.0000	38.6	1.000	0.0773	0.0134	28.6	0.815
0.0041	0.0007	37.7	0.982	0.0898	0.0156	25.8	0.747
0.0093	0.0016	37.4	0.980	0.1223	0.0212	17.2	0.521
0.0150	0.0026	36.8	0.971	0.1395	0.0242	15.2	0.471
0.0221	0.0038	36.1	0.960	0.1656	0.0287	11.7	0.376
0.0359	0.0062	34.5	0.933	0.1932	0.0335	8.38	0.281
0.0556	0.0097	32.0	0.887	0.2004	0.0348	7.19	0.243
T = 358.15 K							
0.0000	0.0000	57.8	1.000	0.0926	0.0161	36.2	0.702
0.0043	0.0007	56.7	0.986	0.1173	0.0203	28.1	0.564
0.0093	0.0016	56.1	0.981	0.1362	0.0236	23.2	0.478
0.0151	0.0026	55.4	0.976	0.1651	0.0286	18.1	0.388
0.0230	0.0040	54.1	0.962	0.1930	0.0335	13.2	0.296
0.0355	0.0062	51.9	0.937	0.2014	0.0349	11.4	0.258
0.0534	0.0093	48.0	0.886	0.2155	0.0374	10.0	0.232
0.0768	0.0133	43.0	0.818				
T = 368.15 K							
0.0000	0.0000	84.4	1.000	0.0928	0.0161	52.8	0.702
0.0043	0.0007	83.0	0.988	0.1111	0.0193	42.1	0.573
0.0094	0.0016	82.2	0.985	0.1320	0.0229	34.2	0.480
0.0147	0.0026	80.9	0.975	0.1611	0.0279	26.0	0.380
0.0230	0.0040	79.2	0.964	0.1948	0.0338	18.2	0.280
0.0353	0.0061	75.9	0.938	0.2008	0.0348	17.4	0.270
0.0522	0.0090	70.4	0.888	0.2159	0.0375	15.5	0.246
0.0747	0.0130	63.1	0.820				

$$w_2 = \frac{m_2}{m_1 + m_2}$$

Standard uncertainties u are as follows: $u(x_1) = 2 \times 10^{-3}$; $u(P) = 0.5$ kPa, $u(T) = 0.05$ K

Br < [N_{1,2OH,2OH,2OH}]Br < [MOR_{1,3}SO₃]. Surprisingly, the increase in polarity increases the activity coefficient of water, this could be explained by weakening the water–LiBr interactions and an increase in the LiBr–organic salt interactions. Simultaneously, water–organic salt interactions are weaker than water–LiBr interactions, thus increasing the water activity coefficients.

Table 6 Experimental and calculated P - x data for the systems {LiBr (1) + [N_{1,2OH,2OH,2OH}]Br (2) + water (3)}, $w_2 = 0.3003$ at different temperatures from 338.15 to 368.15 K; w_2 , (additive to LiBr) mass fraction; x_1 , lithium bromide mole fraction at the equilibrium state; x_2 , additive mole fraction at the equilibrium state; P , equilibrium pressure; T , equilibrium temperature; γ_3 , activity coefficient of water calculated based on the experimental data

x_1	x_2	P (kPa)	γ_3	x_1	x_2	P (kPa)	γ_3
$T = 338.15$ K							
0.0000	0.0000	25.1	1.000	0.0597	0.0100	20.4	0.874
0.0027	0.0004	24.5	0.979	0.0766	0.0128	18.7	0.818
0.0071	0.0012	24.2	0.972	0.0944	0.0158	16.2	0.725
0.0155	0.0026	23.8	0.966	0.1226	0.0205	13.1	0.609
0.0250	0.0042	23.1	0.948	0.1413	0.0236	10.0	0.477
0.0431	0.0072	22.0	0.923	0.1698	0.0284	6.74	0.335
$T = 348.15$ K							
0.0000	0.0000	38.6	1.000	0.0769	0.0128	28.9	0.823
0.0028	0.0005	37.8	0.982	0.0942	0.0157	25.2	0.734
0.0070	0.0012	37.6	0.982	0.1195	0.0200	20.5	0.618
0.0156	0.0026	36.8	0.971	0.1436	0.0240	16.0	0.498
0.0248	0.0041	35.9	0.958	0.1741	0.0291	10.6	0.345
0.0422	0.0070	34.0	0.926	0.2021	0.0337	6.28	0.213
0.0601	0.0100	31.5	0.877				
$T = 358.15$ K							
0.0000	0.0000	57.8	1.000	0.0740	0.0124	43.6	0.825
0.0027	0.0004	56.9	0.987	0.0937	0.0156	37.8	0.734
0.0069	0.0012	56.4	0.984	0.1184	0.0198	31.5	0.632
0.0154	0.0026	55.3	0.974	0.1416	0.0236	24.2	0.501
0.0249	0.0042	53.8	0.959	0.1724	0.0288	16.5	0.357
0.0401	0.0067	51.1	0.928	0.2018	0.0337	10.6	0.240
0.0568	0.0095	47.7	0.884				
$T = 368.15$ K							
0.0000	0.0000	84.4	1.000	0.0726	0.0121	63.7	0.825
0.0027	0.0004	83.2	0.989	0.0921	0.0154	55.7	0.740
0.0070	0.0012	82.4	0.984	0.1178	0.0197	45.6	0.626
0.0152	0.0025	80.9	0.976	0.1450	0.0242	36.0	0.513
0.0247	0.0041	78.9	0.963	0.1753	0.0293	24.7	0.368
0.0396	0.0066	74.8	0.929	0.2058	0.0344	16.2	0.253
0.0579	0.0097	69.8	0.887	0.2241	0.0374	9.48	0.152

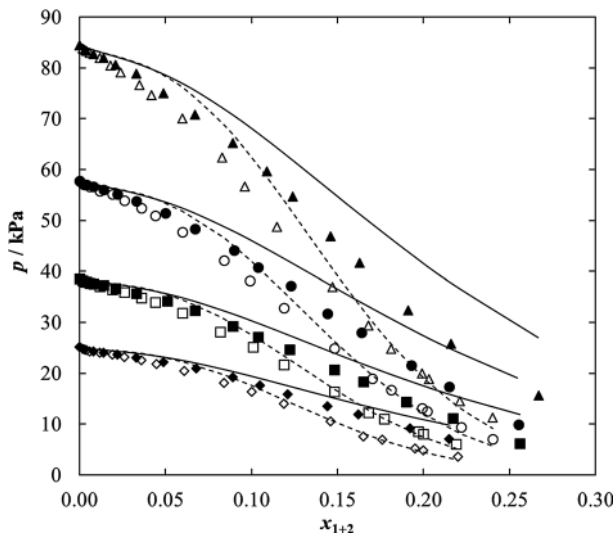
$$w_2 = \frac{m_2}{m_1 + m_2}$$

Standard uncertainties u are as follows: $u(x_1) = 2 \times 10^{-3}$; $u(P) = 0.5$ kPa and $u(T) = 0.05$ K

To our best knowledge, the vapor pressure of {LiBr (1) + additive (2) + water (3)} systems is usually higher than for the vapor pressure of aqueous lithium bromide solutions without any additive at the same conditions, as was reported for the following additives: lithium iodide [14], lithium nitrate [14], ethanolamine [15], 1,3-propanediol [16], sodium formate [19], or potassium formate [19].

It was observed by Luo et al. [22] that the addition of [BMIM][Cl] to {LiNO₃ + H₂O} system results in a higher vapor pressure compared to binary systems without additives, therefore [BMIM][Cl] reduces the absorption ability of LiNO₃/[BMIM][Cl]/H₂O system.

Fig. 2 Experimental and calculated P - x data for the systems {LiBr (1) + [MOR_{1,3}SO₃] (2) + water (3)}, $w_2 = 0.3003$ at different temperatures: filled diamond, 338.15 K; filled square, 348.15 K; filled circle, 358.15 K; filled triangle, 368.15 K. Full points, experimental data for ternary systems; empty points, experimental data for binary system; dotted lines, COSMO RS predictions for binary system; solid lines, COSMO RS predictions for ternary system



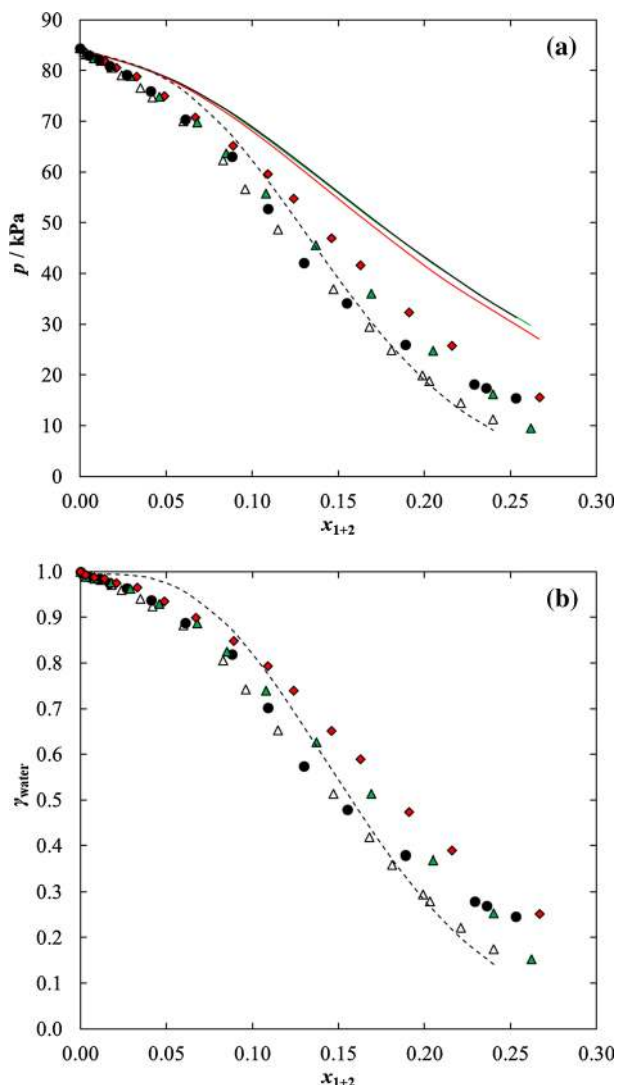
Besides the measured data, Figs. 1, 2 and 3 present the results of the COSMO-RS predictions for the VLE systems studied. Satisfactory predictions are observed for the binary {LiBr+water} system, though the model predictions show significant discrepancies to the experimental data for the systems with the additives. In terms of statistics, one can summarize the results of modelling by means of the average absolute deviations (AADs) between calculated and the measured VLE pressure. The values obtained for each system/additive are as follows (in kPa): 4.8 for [N_{1,2}OH₂OH₂OH]Br, 5.7 for [N_{1,2}OH₂OH]Br, 3.2 [MOR_{1,3}SO₃]. Hence, the deviations are indeed significant if one takes into account that the systems under study displays quite low volatility. For binary {LiBr+water} mixtures, the value of AAD arising from the COSMO-RS calculations is much lower than those for the ternary systems, namely, 1.6 kPa. This finding suggests an accurate modelling of a quantitative effect of an additive on VLE is quite challenging, even when such an advanced thermodynamic model like COSMO-RS is employed.

Nevertheless, the most important finding is that the model reproduces experimentally observed impact of an additive on the vapor pressure. In fact, for all three systems considered in this work, the COSMO-RS predicts that the vapor pressure increases upon addition of the additive as well as that an increase in the vapor pressure becomes more significant as the concentration of the LiBr increases. Even though the overall accuracy of prediction of absolute vapor pressure is rather poor, the quality of the prediction of ratio of vapor pressures before and upon addition of the additive is much better. Such qualitative agreement between the experimental and purely predictive trends is quite promising, so that the COSMO-RS approach may be considered as a tool for screening new additives by modifying the VLE diagrams for the aqueous LiBr solutions.

4.2 Density and Dynamic Viscosity Measurements

The experiments were performed over a wide composition and temperature range from 298.15 to 348.15 K with an increment of 5 K at pressure $P = 0.1$ MPa. The experimental data for aqueous lithium bromide solution are tabulated in Table 7 and graphically presented in Figs. 4 and 5.

Fig. 3 **a** The experimental and calculated VLE data; **b** the experimental activity coefficient of water (γ_3) for {LiBr (1) + additive (2) + water (3)} systems at temperature $T=368.15$ K: filled red diamond, [MOR_{1,3}SO₃] ($w_2=0.3003$); filled circle, [N_{1,1,2OH,2OH}]Br ($w_2=0.2996$); filled green triangle, [N_{1,2OH,2OH,2OH}]Br ($w_2=0.3003$); open triangle, without additive. Points, experimental data; dotted line, COSMO RS predictions for {LiBr + water} system; solid lines, COSMO RS predictions for ternary system (Color figure online)



Due to the solubility of lithium bromide in water at room temperature, it was possible to make the measurements in the given temperature range only in a narrow range of composition, up to $x_1=0.25$. It can be noticed that both density and dynamic viscosity increase with increasing LiBr mole fractions and decrease with increasing temperature. Experimental density and viscosity data are consistent with available literature data, as is confirmed by Fig. 6.

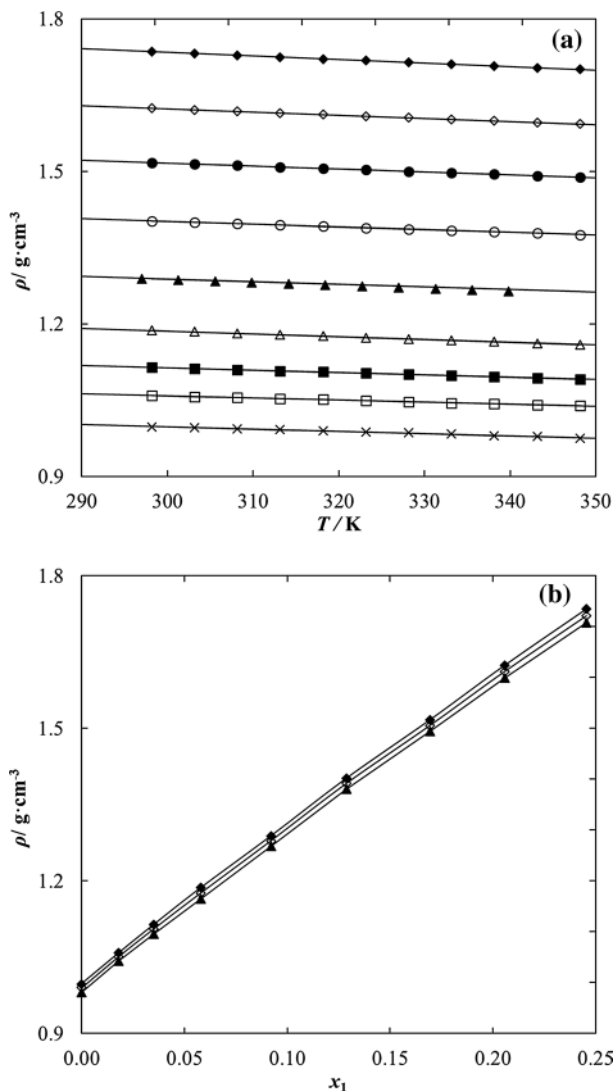
To improve the physicochemical properties, three additives have been added. The additive to lithium bromide mass fraction was exactly the same as in VLE measurements and were as follows: $w_2=0.3003$ for [MOR_{1,3}SO₃]; 0.2996 for [N_{1,1,2OH,2OH}]Br and 0.3003 for [N_{1,2OH,2OH,2OH}]Br. The experimental density and dynamic viscosity data are listed in Tables 8, 9 and 10.

Table 7 The experimental data on liquid density and dynamic viscosity for [LiBr (1) + water (2)] as a function of composition and temperature at pressure $P=0.1$ MPa; x_1 , lithium bromide mole fraction; ρ , liquid density; η , dynamic viscosity; T , temperature

x_1	298.15 K	303.15 K	308.15 K	313.15 K	318.15 K	323.15 K	328.15 K	333.15 K	338.15 K	343.15 K	348.15 K
$\rho/\text{g}\cdot\text{cm}^{-3}$											
0.246	1.7351	1.7316	1.7281	1.7246	1.7211	1.7176	1.7142	1.7107	1.7073	1.7039	1.7004
0.206	1.6241	1.6211	1.6180	1.6149	1.6118	1.6087	1.6055	1.6024	1.5993	1.5962	1.5930
0.170	1.5169	1.5141	1.5114	1.5086	1.5058	1.5029	1.5001	1.4972	1.4943	1.4914	1.4884
0.129	1.4018	1.3993	1.3968	1.3943	1.3917	1.3891	1.3864	1.3837	1.3810	1.3782	1.3754
0.092	1.2887	1.2860	1.2836	1.2813	1.2789	1.2764	1.2739	1.2713	1.2686	1.2659	1.2632
0.058	1.1868	1.1842	1.1812	1.1783	1.1758	1.1727	1.1702	1.1676	1.1650	1.1620	1.1593
0.035	1.1143	1.1120	1.1098	1.1075	1.1053	1.1030	1.1005	1.0981	1.0958	1.0935	1.0914
0.018	1.0590	1.0570	1.0550	1.0531	1.0510	1.0488	1.0468	1.0447	1.0427	1.0408	1.0388
0.000	0.9971	0.9957	0.9940	0.9922	0.9902	0.9879	0.9857	0.9832	0.9803	0.9781	0.9748
$\eta/\text{mPa}\cdot\text{s}$											
0.246	9.066	8.028	7.154	6.410	5.769	5.198	4.695	4.245	3.896	3.574	3.384
0.206	5.202	4.669	4.221	3.841	3.512	3.225	2.974	2.768	2.559	2.370	2.252
0.170	3.258	2.945	2.683	2.459	2.263	2.093	1.943	1.829	1.736	1.643	1.575
0.129	2.164	1.972	1.806	1.662	1.536	1.427	1.330	1.240	1.173	1.110	1.069
0.092	1.601	1.452	1.327	1.219	1.126	1.045	0.975	0.906	0.850	0.810	0.780
0.058	1.307	1.185	1.084	0.998	0.922	0.857	0.793	0.747	0.708	0.674	0.653
0.035	1.161	1.052	0.966	0.888	0.822	0.763	0.716	0.678	0.636	0.603	0.582
0.018	1.019	0.916	0.832	0.764	0.705	0.656	0.607	0.574	0.541	0.515	0.491
0.000	0.890	0.797	0.719	0.653	0.596	0.547	0.504	0.466	0.433	0.404	0.378

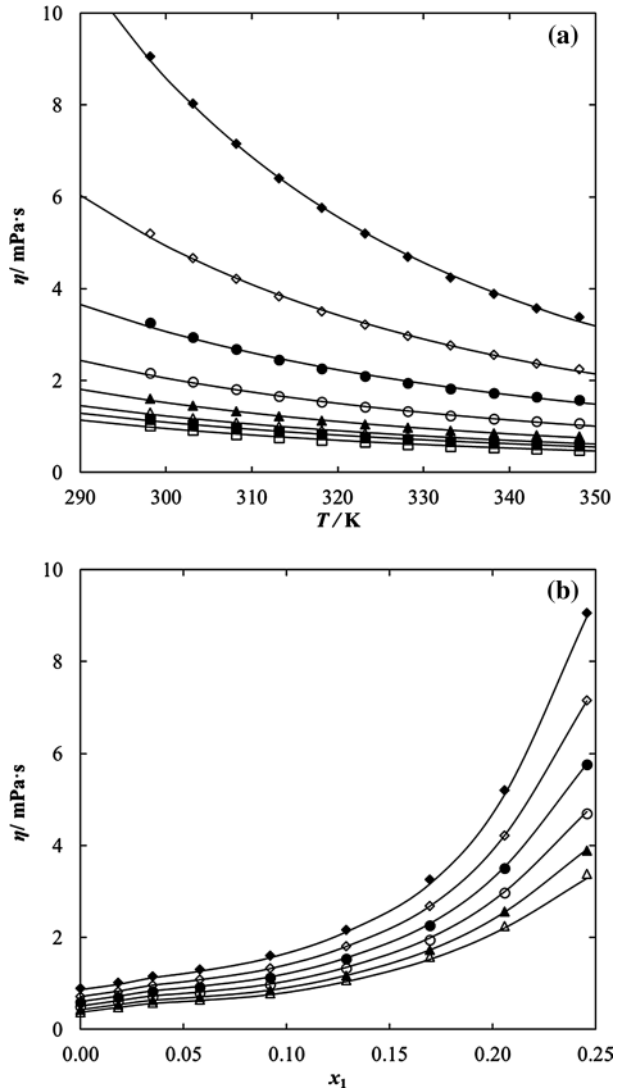
The experimental uncertainties are as follows: $u(x_1)=1 \times 10^{-3}$; $u(\rho)=5 \times 10^{-4} \text{ g}\cdot\text{cm}^{-3}$; $u(\eta)=5\%$, $u(T)=0.01 \text{ K}$; $u(p)=3 \text{ kPa}$

Fig. 4 Experimental and calculated liquid density data for {LiBr (1) + water (2)} binary system **a** as a function of temperature for different LiBr mole fraction, x_1 : filled diamond, 0.246; open diamond, 0.206; filled circle, 0.170; open circle, 0.129; filled triangle, 0.092; open triangle, 0.058; filled square, 0.035; open square, 0.018; x, 0.000; **b** as a function of lithium bromide mole fraction at different temperatures: filled diamond, 298.15 K; open diamond, 318.15 K; filled triangle, 338.15 K. Points, experimental data; solid lines, correlation using Eq. 1 with parameters given in Table 11



The same trends as for aqueous lithium bromide solutions, i.e. an increase in density and viscosity with an increase in composition (x_{1+2}) and a decrease in temperature increase were observed. As an example, the experimental and calculated density data for {LiBr (1) + [MOR_{1,3}SO₃] (2) + water (3)} are graphically presented in Fig. 7. The data for other ternary systems are presented in Figs. S5 and S6 in the supplementary material. It has been shown that each of the tested additives significantly reduces the density compared to the {LiBr + water} system. The comparison of the influence of the tested additives on the density of aqueous lithium bromide solution is shown in Fig. 8. The lowest density was obtained when [MOR_{1,3}SO₃] was used as an additive. The lowest impact on density was observed for [N_{1,2OH,2OH,2OH}]Br, although the density of the system is still lower than for the aqueous lithium bromide solution without the use of an additive.

Fig. 5 Experimental and calculated dynamic viscosity data for the {LiBr (1) + water (2)} binary system **a** as a function of temperature for different LiBr mole fraction, x_1 : filled diamond, 0.246; open diamond, 0.206; filled circle, 0.170; open circle, 0.129; filled triangle, 0.092; open triangle, 0.058; filled square, 0.035; open square, 0.018; x_1 , 0.000; **b** as a function of lithium bromide mole fraction at different temperatures: filled diamond, 298.15 K; open diamond, 308.15 K; filled circle, 318.15 K; open circle, 328.15 K; filled triangle, 338.15 K; open triangle, 348.15 K. Points, experimental data; solid lines, correlation using Eq. 3 with parameters given in Table 12



The decrease of the density of aqueous lithium bromide solution in the presence of the additives is confirmed in the literature. Such a trend was observed with ethanolamine [26], potassium acetate [27], sodium lactate [27], or diethanolamine [28].

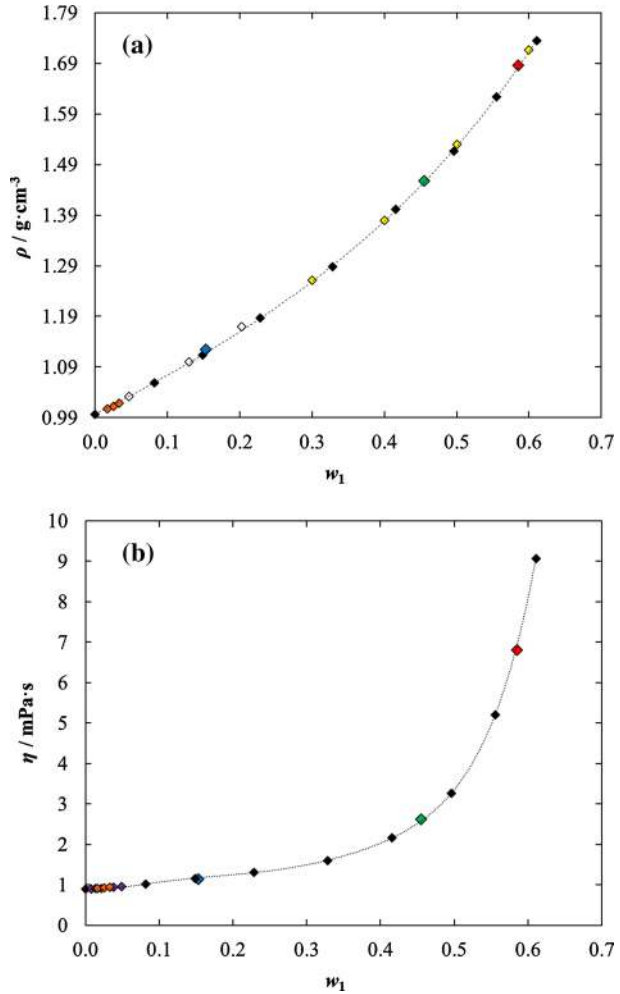
The experimental data has been correlated using the following equation:

$$\rho = \rho_0 \exp[-\alpha_p(T - T_0)], \quad T_0 = 298.15 \text{ K} \quad (1)$$

The root mean square error (RMSE) is expressed by Eq. 2

$$RMSE = \sqrt{\frac{\sum_{i=1}^N (\rho^{\text{calc}} - \rho^{\text{exp}})^2}{N - 2}} \quad (2)$$

Fig. 6 Experimental and literature data on **a** liquid density and **b** dynamic viscosity of {LiBr (1)+ water (2)} binary system at temperature $T=298.15$ K: filled diamond, experimental data; filled red diamond, Ref. [55] at $T=298.09$ K; filled green diamond, Ref. [55] at $T=298.13$ K; filled blue diamond, Ref. [55] at $T=298.12$ K; filled yellow diamond, Ref. [56]; open diamond, Ref. [57]; filled purple diamond, Ref. [58]; filled red diamond [59]. Dotted lines are simply a guide to the eye (Color figure online)



The value of the parameters ρ_0 and α_ρ along with RMSE are collected in Table 11. The maximum RMSE value between the experimental density data and calculated values was determined to be 0.0009, exhibiting excellent consistency and accuracy. The measured data and calculated fitted curves from Eq. 1 are plotted against temperature, or composition in Figs. 4, 6 and 8 as well as in Figs. S5 and S6 in the supplementary material.

Temperature dependence of the dynamic viscosity for {LiBr (1)+ additive (2)+ water (3)} were described using the following Andrade-type equation:

$$\ln \eta / \text{mPa} \cdot \text{s} = A - \frac{B}{T/\text{K}} \quad (3)$$

The root mean square deviation (RMSE) is expressed by Eq. 4

$$RMSE = \sqrt{\frac{\sum_{i=1}^N (\eta^{\text{calc}} - \eta^{\text{exp}})^2}{N - 2}} \quad (4)$$

Table 8 The experimental data on liquid density (ρ) and dynamic viscosity (η) for {LiBr (1) + [MOR_{1.3}SO₃] (2) + water (3)} system, $w_2 = 0.3003$ as a function of composition (x_1) and temperature (T) at pressure $P = 0.1$ MPa; x_1 , lithium bromide mole fraction; x_2 , additive mole fraction; ρ , liquid density; η , dynamic viscosity; T , temperature

x_1	x_2	298.15 K	303.15 K	308.15 K	313.15 K	318.15 K	323.15 K	328.15 K	333.15 K	338.15 K	343.15 K	348.15 K
$\rho/\text{g}\cdot\text{cm}^{-3}$												
	0.242	1.6337	1.6312	1.6287	1.6262	1.6236	1.6210	1.6184	1.6158	1.6132	1.6105	1.6078
	0.215	1.5827	1.5803	1.5778	1.5753	1.5728	1.5703	1.5677	1.5651	1.5625	1.5599	1.5573
	0.191	1.5353	1.5329	1.5304	1.5279	1.5254	1.5229	1.5204	1.5178	1.5152	1.5126	1.5100
	0.164	1.4782	1.4758	1.4734	1.4710	1.4685	1.4660	1.4635	1.4609	1.4583	1.4557	1.4531
	0.138	1.4161	1.4137	1.4114	1.4089	1.4065	1.4040	1.4015	1.3989	1.3964	1.3937	1.3910
	0.111	1.3506	1.3483	1.3460	1.3436	1.3412	1.3388	1.3362	1.3336	1.3310	1.3281	1.3249
	0.083	1.2740	1.2719	1.2696	1.2674	1.2650	1.2626	1.2600	1.2574	1.2544	1.2512	1.2489
	0.060	1.2071	1.2051	1.2030	1.2007	1.1984	1.1953	1.1920	1.1895	1.1870	1.1834	1.1803
	0.034	1.1230	1.1212	1.1192	1.1171	1.1155	1.1132	1.1111	1.1090	1.1070	1.1051	1.1030
	0.009	1.0319	1.0303	1.0281	1.0260	1.0239	1.0211	1.0191	1.0169	1.0150	1.0129	1.0111
$\eta/\text{mPa}\cdot\text{s}$												
	0.242	96.708	81.443	66.635	55.287	46.289	39.453	33.680	29.979	26.203	22.809	20.432
	0.215	33.380	28.070	23.693	20.290	17.528	15.257	13.424	11.871	10.579	9.650	8.450
	0.191	17.791	16.381	14.191	12.392	10.870	9.544	8.465	7.546	6.750	6.231	5.629
	0.164	9.666	8.497	7.559	6.659	5.888	5.294	4.804	4.356	4.052	3.644	3.299
	0.138	5.562	4.871	4.353	3.907	3.539	3.220	2.935	2.729	2.482	2.307	2.088
	0.111	3.315	3.049	2.740	2.481	2.278	2.090	1.926	1.795	1.661	1.539	1.421
	0.083	0.014	2.238	2.045	1.694	1.555	1.440	1.351	1.268	1.189	1.103	1.025
	0.060	0.010	1.655	1.514	1.389	1.264	1.075	1.007	0.935	0.881	0.824	0.763
	0.034	0.006	1.117	1.012	0.926	0.852	0.790	0.734	0.687	0.646	0.604	0.572
	0.009	0.002	0.953	0.877	0.797	0.674	0.625	0.584	0.549	0.520	0.482	0.453

The experimental uncertainties are as follows: $u(x_1) = 1 \times 10^{-3}$; $u(\rho) = 5 \times 10^{-4}$ g·cm⁻³; $u(\eta) = 5\%$; $u(T) = 0.01$ K; $u(p) = 3$ kPa

Table 9 The experimental data on liquid density (ρ) and dynamic viscosity (η) for {LiBr (1) + [N_{1,1,1,2,2,2,2}][Br (2) + water (3)] system, $w_2 = 0.2996$ as a function of composition (x_1) and temperature (T) at pressure $P = 0.1$ MPa; x_1 , lithium bromide mole fraction; x_2 , additive mole fraction; ρ , liquid density; η , dynamic viscosity; T , temperature

x_1	x_2	298.15 K	303.15 K	308.15 K	313.15 K	318.15 K	323.15 K	328.15 K	333.15 K	338.15 K	343.15 K	348.15 K
$\rho/\text{g}\cdot\text{cm}^{-3}$												
	0.247	1.6699	1.6671	1.6643	1.6616	1.6588	1.6560	1.6532	1.6503	1.6475	1.6447	1.6418
	0.222	1.6211	1.6184	1.6157	1.6130	1.6102	1.6075	1.6047	1.6020	1.5992	1.5964	1.5936
	0.196	1.5659	1.5633	1.5607	1.5580	1.5554	1.5527	1.5500	1.5473	1.5446	1.5418	1.5391
	0.170	1.5083	1.5058	1.5032	1.5006	1.4980	1.4954	1.4927	1.4900	1.4873	1.4846	1.4819
	0.145	1.4450	1.4426	1.4400	1.4375	1.4348	1.4322	1.4295	1.4268	1.4240	1.4211	1.4181
	0.119	1.3816	1.3792	1.3768	1.3743	1.3718	1.3693	1.3667	1.3641	1.3614	1.3587	1.3557
	0.094	1.3119	1.3097	1.3074	1.3050	1.3026	1.3000	1.2975	1.2952	1.2928	1.2901	1.2873
	0.068	1.2366	1.2345	1.2323	1.2300	1.2276	1.2253	1.2231	1.2211	1.2190	1.2170	1.2150
	0.043	1.1537	1.1518	1.1498	1.1478	1.1457	1.1437	1.1417	1.1398	1.1378	1.1359	1.1340
	0.017	1.0647	1.0630	1.0613	1.0597	1.0579	1.0561	1.0549	1.0532	1.0515	1.0501	1.0491
$\eta/\text{mPa}\cdot\text{s}$												
	0.247	40.761	33.989	28.429	23.855	20.769	17.871	15.658	13.795	12.147	10.843	9.314
	0.222	20.868	17.691	15.179	13.190	11.525	10.174	9.015	8.048	7.220	6.430	6.146
	0.196	11.552	10.028	8.831	7.828	6.985	6.275	5.653	5.103	4.623	4.281	3.982
	0.170	6.402	5.677	5.063	4.553	4.123	3.760	3.448	3.172	2.928	2.740	2.644
	0.145	4.076	3.658	3.302	3.004	2.755	2.537	2.346	2.198	2.076	1.987	1.951
	0.119	2.847	2.559	2.320	2.117	1.942	1.793	1.661	1.544	1.448	1.348	1.297
	0.094	2.071	1.868	1.698	1.556	1.432	1.324	1.233	1.150	1.081	1.043	1.006
	0.068	1.648	1.492	1.359	1.244	1.145	1.062	0.983	0.932	0.860	0.832	0.805
	0.043	1.323	1.191	1.084	0.990	0.912	0.849	0.793	0.743	0.698	0.652	0.613
	0.017	1.062	0.955	0.867	0.794	0.735	0.685	0.635	0.596	0.564	0.553	0.537

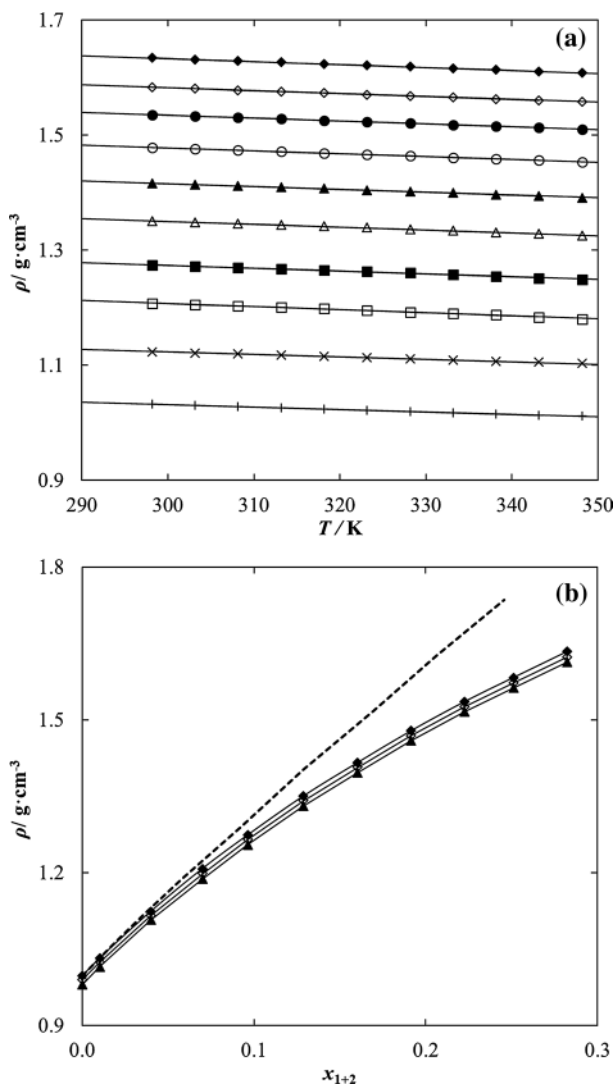
The experimental uncertainties are as follows: $u(x_1) = 1 \times 10^{-3}$; $u(\rho) = 5 \times 10^{-4}$ g·cm⁻³; $u(\eta) = 5\%$; $u(T) = 0.01$ K; $u(p) = 3$ kPa

Table 10 The experimental data on liquid density (ρ) and dynamic viscosity (η) for $\{\text{LiBr} (1) + [\text{N}_{1.20\text{H}_{2.01\text{H}_{2.01}}]\text{Br} (2) + \text{water} (3)\}$ system, $w_2 = 0.3003$ as a function of composition (x_1) and temperature (T) at pressure $P=0.1$ MPa. x_1 , lithium bromide mole fraction; x_2 , additive mole fraction; ρ , liquid density; η , dynamic viscosity; T , temperature

x_1	x_2	298.15 K	303.15 K	308.15 K	313.15 K	318.15 K	323.15 K	328.15 K	333.15 K	338.15 K	343.15 K	348.15 K
$\rho/\text{g}\cdot\text{cm}^{-3}$	0.267	1.7192	1.7164	1.7135	1.7107	1.7078	1.7050	1.7022	1.6993	1.6964	1.6936	1.6907
	0.240	1.6679	1.6651	1.6623	1.6596	1.6568	1.6540	1.6512	1.6484	1.6456	1.6428	1.6399
	0.215	1.6164	1.6137	1.6110	1.6083	1.6055	1.6028	1.6001	1.5973	1.5945	1.5918	1.5890
	0.188	1.5580	1.5554	1.5527	1.5501	1.5474	1.5447	1.5420	1.5393	1.5366	1.5338	1.5311
	0.163	1.4996	1.4970	1.4944	1.4918	1.4892	1.4866	1.4839	1.4812	1.4785	1.4758	1.4730
	0.137	1.4348	1.4323	1.4298	1.4273	1.4247	1.4221	1.4195	1.4169	1.4142	1.4115	1.4087
	0.111	1.3626	1.3602	1.3578	1.3553	1.3528	1.3503	1.3477	1.3450	1.3423	1.3395	1.3367
	0.086	1.2948	1.2926	1.2903	1.2879	1.2855	1.2830	1.2805	1.2779	1.2752	1.2725	1.2697
	0.060	1.2147	1.2127	1.2105	1.2083	1.2059	1.2035	1.2010	1.1984	1.1958	1.1930	1.1902
	0.026	1.0987	1.0970	1.0951	1.0930	1.0908	1.0885	1.0861	1.0835	1.0807	1.0779	1.0741
$\eta/\text{mPa}\cdot\text{s}$	0.267	77.386	62.737	54.128	45.304	38.579	33.316	28.960	25.348	22.402	20.030	18.918
	0.240	40.585	33.892	28.438	24.318	21.123	18.329	16.325	14.407	12.782	11.449	10.048
	0.215	17.914	15.358	13.311	11.632	10.259	9.105	8.118	7.304	6.511	5.848	5.280
	0.188	9.806	8.587	7.573	6.721	6.010	5.408	4.889	4.440	4.055	3.717	3.425
	0.163	5.976	5.303	4.470	4.268	3.857	3.510	3.210	2.948	2.722	2.521	2.345
	0.137	3.933	3.532	3.191	2.920	2.691	2.485	2.330	2.184	2.070	1.960	1.877
	0.111	2.660	2.401	2.173	1.981	1.822	1.684	1.573	1.474	1.387	1.307	1.245
	0.086	2.012	1.817	1.651	1.514	1.401	1.307	1.221	1.147	1.078	1.018	0.949
	0.060	1.574	1.413	1.287	1.184	1.094	1.010	0.951	0.892	0.837	0.791	0.740
	0.026	1.143	1.029	0.935	0.856	0.791	0.731	0.683	0.641	0.603	0.572	0.550

The experimental uncertainties are as follows: $u(x_1) = 1 \times 10^{-3}$; $u(\rho) = 5 \times 10^{-4}$ g·cm⁻³; $u(\eta) = 5\%$; $u(T) = 0.01$ K; $u(P) = 3$ kPa

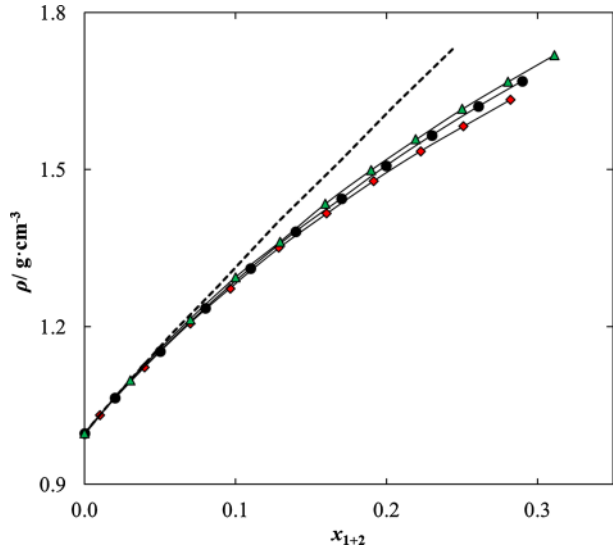
Fig. 7 Experimental and calculated liquid density data for {LiBr (1) + [MOR_{1,3}SO₃] (2) + water (3)}, ($w_2=0.3003$), as a function of **a** temperature for different compositions (x_{1+2}): filled diamond, 0.282; open diamond, 0.251; filled circle, 0.223; open circle, 0.191; filled triangle, 0.160; open triangle, 0.129; filled square, 0.097; open square, 0.070; multiplication sign, 0.040; plus sign, 0.010; **b** composition at different temperature, T : filled diamond, 298.15 K; open diamond, 318.15 K; filled triangle, 338.15 K. Points, experimental results, solid lines, calculated using Eq. 1 with parameters given in Table 11; dotted line, experimental data for {LiBr (1) + water (2)} binary system at $T=298.15$ K



The values of parameters A and B , along with RMSE are collected in Table 12.

As an example, the experimental and calculated dynamic viscosity for the {LiBr (1) + [MOR_{1,3}SO₃] (2) + water (3)} ternary systems as a function of temperature and composition are presented in Fig. 9. Data for the other two systems is presented in Figs. S7 and S8 in the supplementary material. In these figures, the dynamic viscosities for aqueous lithium bromide solutions without additive at 298.15 K are marked in dashed lines. In each case, the presence of the additive causes an increase in the viscosity of the system, which is unfavorable for use in absorption refrigeration technology. Increasing the viscosity of the refrigeration system is associated with greater energy expenditure related to the transport of the cooling medium in the system. The increase in the viscosity of the refrigeration system by adding a third component (additive) is confirmed in the literature [26, 28, 31].

Fig. 8 The experimental and calculated liquid density data for {LiBr (1) + additive (2) + water (3)} as a function of composition at temperature $T=298.15$ K: filled red diamond, $[\text{MOR}_{1,3}\text{SO}_3]$ ($w_2=0.3003$); filled circle, $[\text{N}_{1,1,2\text{OH},2\text{OH}}]\text{Br}$ ($w_2=0.2996$); filled green triangle, $[\text{N}_{1,2\text{OH},2\text{OH},2\text{OH}}]\text{Br}$ ($w_2=0.3003$). Points, experimental results; solid lines, calculation using Eq. 1 with parameters given in Table 11, dotted line, density data for {LiBr (1) + water (2)} binary system (Color figure online)



A comparison of the influence of all additives tested in this work on the dynamic viscosity of the working fluid is shown in Fig. 10. It can be noticed that the viscosity of the {LiBr (1) + additive (2) + water (3)} systems increases when the following additives are used: $[\text{MOR}_{1,3}\text{SO}_3] > [\text{N}_{1,2\text{OH},2\text{OH},2\text{OH}}]\text{Br} > [\text{N}_{1,1,2\text{OH},2\text{OH}}]\text{Br}$. To sum up, the lowest viscosity of the system was obtained for the system with $[\text{N}_{1,1,2\text{OH},2\text{OH}}]\text{Br}$ as an additive, but these values are higher than for conventional working fluid without any additives.

5 Conclusion

In this work, the vapor pressures, liquid densities and dynamic viscosities for the {LiBr + additive + water} systems with (additive to LiBr) mass fraction, $w_2=0.3$ were measured over a wide composition range at various temperatures. To verify the experimental method, these properties were also measured for aqueous lithium bromide solution and were consistent with available literature data.

The three ternary systems: {LiBr + $[\text{MOR}_{1,3}\text{SO}_3]$ + water}, {LiBr + $[\text{N}_{1,1,2\text{OH},2\text{OH}}]\text{Br}$ + water} and {LiBr + $[\text{N}_{1,2\text{OH},2\text{OH},2\text{OH}}]\text{Br}$ + water} were considered as possible new working fluids for absorption refrigeration technology. Results show that the vapor pressure for the ternary systems is higher than for the working fluid without any additives. The relative trend of the effect on the VLE data was successfully predicted by using the COSMO-RS model. Both density and dynamic viscosity of the tested binary and ternary systems decrease with increasing temperature and increase with increasing salt concentration. The densities of the tested ternary systems are lower than that of the aqueous lithium bromide solutions. In contrast, the presence of the additive increases the viscosity of the systems. The data and correlation information presented in this study are important for the design of refrigeration equipment using this new generation of working fluids.

Table 11 The parameters of Eqs. 1 and 2 for correlation temperature dependence of the density of {LiBr (1) + water (2)} and {LiBr (1) + additive (2) + water (3)} systems

x_1 , or x_{1+2}	$\rho_0/\text{g}\cdot\text{cm}^{-3}$	$10^4 \alpha_p/\text{K}^{-1}$	$10^3 \cdot \sigma/\text{g}\cdot\text{cm}^{-3}$
{LiBr (1) + water (2)}			
0.2456	1.73508	4.0	0.02
0.2058	1.62423	3.9	0.06
0.1695	1.51708	3.8	0.13
0.1288	1.40213	3.8	0.22
0.0920	1.28880	4.0	0.23
0.0578	1.18680	4.7	0.15
0.0350	1.11438	4.2	0.12
0.0180	1.05908	3.9	0.07
{LiBr (1) + [MOR _{1,3} SO ₃] (2) + water (3)}, $w_2=0.3003$			
0.2823	1.63373	3.2	0.23
0.2512	1.58294	3.2	0.29
0.2226	1.53540	3.3	0.16
0.1914	1.47824	3.4	0.22
0.1604	1.41606	3.5	0.29
0.1289	1.35058	3.7	0.56
0.0966	1.27450	3.9	0.62
0.0700	1.20790	4.4	0.80
0.0399	1.12404	3.9	0.56
0.0102	1.03243	4.2	0.35
{LiBr (1) + [N _{1,1,2OH,2OH}]Br (2) + water (3)}, $w_2=0.2996$			
0.2898	1.66987	3.4	0.19
0.2607	1.62124	3.4	0.16
0.2299	1.56615	3.5	0.18
0.1999	1.50846	3.6	0.38
0.1701	1.44534	3.8	0.41
0.1397	1.38204	3.8	0.30
0.1100	1.31240	3.8	0.24
0.0799	1.23663	3.5	0.40
0.0499	1.15383	3.5	0.09
0.0203	1.06465	3.0	0.35
{LiBr (1) + [N _{1,2OH,2OH,2OH}]Br (2) + water (3)}, $w_2=0.3003$			
0.3111	1.71921	3.3	0.20
0.2803	1.66799	3.4	0.12
0.2503	1.61644	3.4	0.11
0.2195	1.55801	3.5	0.23
0.1899	1.49970	4.0	0.23
0.1595	1.43519	3.7	0.19
0.1297	1.36313	3.9	0.34
0.1002	1.29554	4.0	0.38
0.0700	1.21566	4.2	0.52
0.0305	1.10033	4.5	0.91

$$\rho = \rho_0 \exp[-\alpha_p(T - T_0)], \quad T_0 = 298.15 \text{ K}$$

$$RMSE = \sqrt{\frac{\sum_{i=1}^N (\rho^{\text{calc}} - \rho^{\text{exp}})^2}{N-2}}$$

Table 12 The parameters of Eqs. 3 and 4 for correlation temperature dependence of the dynamic viscosity of {LiBr (1) + additive (2) + water (3)} systems

x_1 , or x_{1+2}	A	$10^{-3}B/K$	$\sigma/\text{mPa}\cdot\text{s}$
{LiBr (1) + water (2)}			
0.2456	– 4.800	– 17.338	0.05
0.2058	– 4.221	– 14.511	0.04
0.1695	– 3.949	– 12.648	0.05
0.1288	– 4.238	– 12.372	0.02
0.0920	– 4.639	– 12.615	0.02
0.0578	– 4.681	– 12.202	0.02
0.0350	– 4.720	– 12.005	0.01
0.0180	– 5.084	– 12.569	0.02
{LiBr (1) + [MOR _{1,3} SO ₃] (2) + water (3)}, $w_2=0.3003$			
0.2823	– 6.380	– 27.095	1.32
0.2512	– 5.984	– 23.456	0.42
0.2226	– 5.396	– 20.581	0.25
0.1914	– 5.160	– 18.384	0.07
0.1604	– 4.958	– 16.488	0.05
0.1289	– 4.692	– 14.603	0.02
0.0966	– 4.553	– 13.253	0.02
0.0700	– 4.845	– 13.241	0.01
0.0399	– 5.065	– 13.002	0.01
0.0102	– 5.206	– 12.761	0.01
{LiBr (1) + [N _{1,1,2OH,2OH}]Br (2) + water (3)}, $w_2=0.2996$			
0.2898	– 6.400	– 24.988	0.47
0.2607	– 5.717	– 21.632	0.24
0.2299	– 5.033	– 18.483	0.11
0.1999	– 4.455	– 15.574	0.09
0.1701	– 3.923	– 13.114	0.08
0.1397	– 4.503	– 13.701	0.03
0.1100	– 4.427	– 12.702	0.03
0.0799	– 4.632	– 12.653	0.02
0.0499	– 5.011	– 13.057	0.01
0.0203	– 4.830	– 12.018	0.02
{LiBr (1) + [N _{1,2OH,2OH,2OH}]Br (2) + water (3)}, $w_2=0.3003$			
0.3111	– 5.680	– 24.749	1.34
0.2803	– 5.872	– 23.651	0.56
0.2503	– 5.559	– 20.890	0.12
0.2195	– 5.049	– 18.129	0.08
0.1899	– 4.708	– 16.049	0.06
0.1595	– 3.808	– 12.745	0.07
0.1297	– 4.336	– 13.106	0.04
0.1002	– 4.438	– 12.673	0.02
0.0700	– 4.715	– 12.746	0.02
0.0305	– 5.017	– 12.691	0.02

$$\ln\eta/\text{mPa}\cdot\text{s} = A - \frac{B}{T/\text{K}}$$

$$RMSE = \sqrt{\frac{\sum_{i=1}^N (\eta^{\text{calc}} - \eta^{\text{exp}})^2}{N-2}}$$

Fig. 9 Experimental and calculated dynamic viscosity data for {LiBr (1) + [MOR_{1,3}SO₃] (2) + water (3)}, $w_2 = 0.3003$, as a function of **a** temperature for different compositions (x_{1+2}): filled diamond, 0.282; open diamond, 0.251; filled circle, 0.223; open circle, 0.191; filled triangle, 0.160; open triangle, 0.129; filled square, 0.097; open square, 0.070; multiplication sign, 0.040; plus sign, 0.010; **b** composition at different temperature, T : filled diamond, 298.15 K; open diamond, 318.15 K; filled diamond, 338.15 K. Points, experimental results, solid lines, calculated using Eq. 3 with parameters given in Table 12; dotted line, experimental data for {LiBr (1) + water (2)} binary system at $T = 298.15$ K

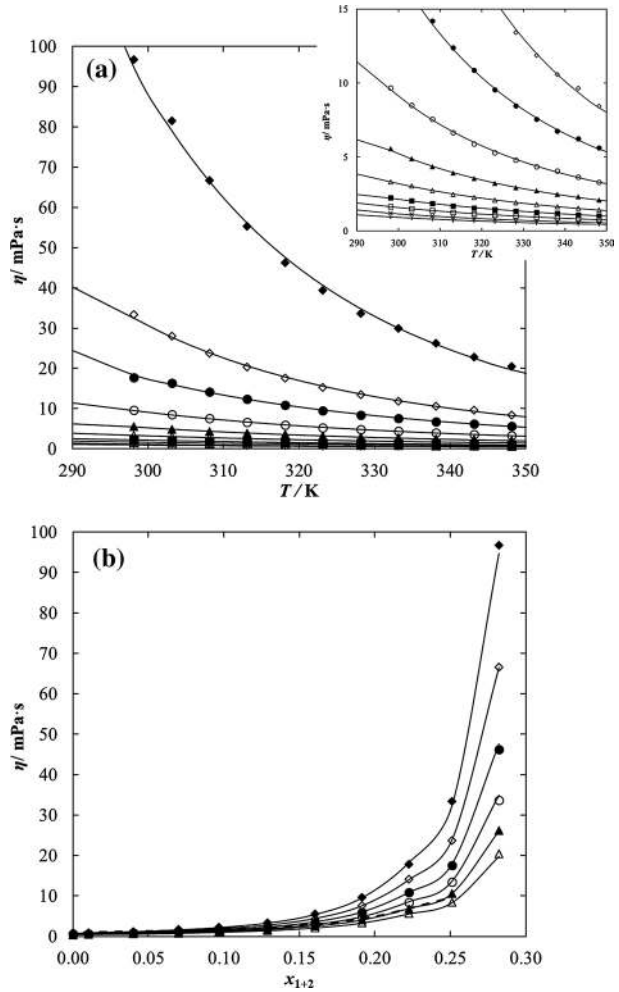
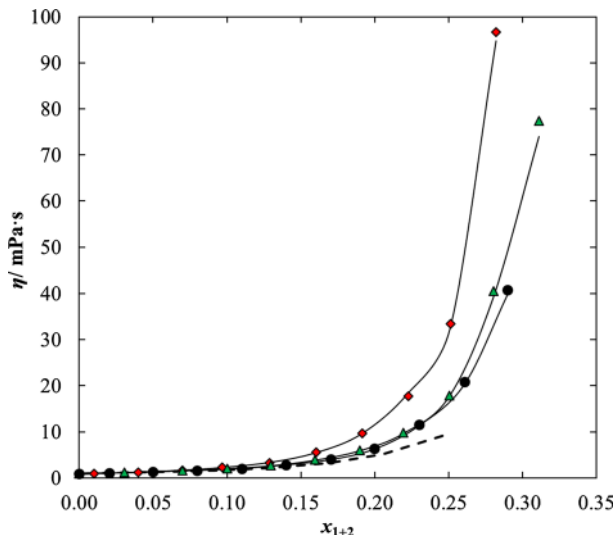


Fig. 10 The experimental and calculated dynamic viscosity data for {LiBr (1)+ additive (2)+ water (3)} as a function of composition at temperature $T=298.15$ K: filled red diamond, $[\text{MOR}_{1,3}\text{SO}_3]$ ($w_2=0.3003$); filled circle, $[\text{N}_{1,1,2\text{OH},2\text{OH}}]$ Br ($w_2=0.2996$); filled green triangle, $[\text{N}_{1,2\text{OH},2\text{OH},2\text{OH}}]$ Br ($w_2=0.3003$). Points, experimental results; solid lines, calculation using Eq. 3 with parameters given in Table 12, dotted line, dynamic viscosity data for {LiBr (1)+ water (2)} binary system (Color figure online)



Supplementary Information The online version contains supplementary material available at <https://doi.org/10.1007/s10953-021-01071-w>.

Acknowledgements Funding for this research was provided by the Ministry of Science and Higher Education in the years 2016–2019 within the framework of the Project “Iuventus Plus” No. 379/IP3/2016/74. This work has been partially financed by Warsaw University of Technology.

Open Access This article is licensed under a Creative Commons Attribution 4.0 International License, which permits use, sharing, adaptation, distribution and reproduction in any medium or format, as long as you give appropriate credit to the original author(s) and the source, provide a link to the Creative Commons licence, and indicate if changes were made. The images or other third party material in this article are included in the article’s Creative Commons licence, unless indicated otherwise in a credit line to the material. If material is not included in the article’s Creative Commons licence and your intended use is not permitted by statutory regulation or exceeds the permitted use, you will need to obtain permission directly from the copyright holder. To view a copy of this licence, visit <http://creativecommons.org/licenses/by/4.0/>.

References

- Zhuo, C.Z., Machielsen, C.H.M.: Thermophysical properties of the trifluoroethanol-pyrrolidone system for absorption heat transformers. *Int. J. Refrig.* **16**, 357–363 (1993)
- Srikhirin, P., Aphornratana, S., Chungpaibulpatana, S.: A review of absorption refrigeration technologies. *Renew. Sust. Energy Rev.* **5**, 343–372 (2001)
- Aphornratana, S., Chungpaibulpatana, S., Srikhirin, P.: Experimental investigation of an ejector refrigerator: effect of mixing chamber geometry on system performance. *Int. J. Energy Res.* **25**, 397–411 (2001)
- Khamooshi, M., Parham, K., Atikol, U.: Overview of ionic liquids used as working fluids in absorption cycles. *Adv. Mech. Eng.* **2013**, 1–7 (2013)
- Mark, B.S., Yokozeki, A.: Absorption cycle using ionic liquids as working fluids. *US2006/0197053 A1* (2006)
- Dong, L., Zheng, D.X., Wei, Z., Wu, X.H.: Synthesis of 1,3-dimethylimidazolium chloride and volumetric property investigations of its aqueous solution. *Int. J. Thermophys.* **30**, 1480–1490 (2009)
- Nie, N., Zheng, D., Dong, L., Li, Y.: Thermodynamic properties of the water + 1-(2-hydroxyethyl)-3-methylimidazolium chloride system. *J. Chem. Eng. Data* **57**, 3598–3603 (2012)

8. Zheng, D., Dong, L., Huang, W., Wu, X., Nie, N.A.: A review of imidazolium ionic liquids research and development towards working pair of absorption cycle. *Renew. Sust. Energy Rev.* **37**, 47–68 (2014)
9. Królikowska, M., Padaszyński, K., Zawadzki, M.: (Vapor + liquid) phase equilibria of an aqueous solution of bromide-based ionic liquids—measurements, correlations and application to absorption cycles. *Fluid Phase Equilib.* **494**, 201–211 (2019)
10. Kim, S., Kohl, P.A.: Analysis of [hmim][PF₆] and [hmim][Tf₂N] ionic liquids as absorbents for an absorption refrigeration system. *Int. J. Refrig.* **48**, 105–113 (2014)
11. Boryta, D.A.: Solubility of lithium bromide in water between 50° and +100°C. (45 to 70% lithium bromide). *J. Chem. Eng. Data* **15**, 142–144 (1970)
12. Iyoki, S., Uemura, T.: Vapour pressure of the water–lithium bromide system and the water–lithium bromide–zinc bromide–lithium chloride system at high temperatures. *Int. J. Refrig.* **12**, 278–282 (1989)
13. Iyoki, S., Hisashi Gouda, A., Uemura, T.: Heat capacities of ethylamine + water + lithium bromide from 313.15 K to 373.15 K. *J. Chem. Eng. Data* **43**, 893–894 (1998)
14. Iyoki, S., Iwasaki, S., Kuriyama, Y., Uemura, T.: Densities, viscosities, and surface tensions for the two ternary systems H₂O + LiBr + LiI and H₂O + LiCl + LiNO₃. *J. Chem. Eng. Data* **38**, 302–305 (1993)
15. Kim, J.-S., Park, Y., Lee, H.: Solubilities and vapor pressures of the water + lithium bromide + ethanolamine system. *J. Chem. Eng. Data* **41**, 279–281 (1996)
16. Kim, J.-S., Park, Y., Lee, H.: Physical properties of the lithium bromide + 1,3-propanediol + water system. *Int. J. Refrig.* **20**, 319–325 (1997)
17. Kim, J.-S., Park, Y., Lee, H., Yu, S.I.: Heat capacities of the water + lithium bromide + ethanolamine and water + lithium bromide + 1, 3-propanediol systems. *J. Chem. Eng. Data* **42**, 371–373 (1997)
18. Park, Y., Kim, J.-S., Lee, H., Yu, S.J.: Density, vapor pressure, solubility and viscosity for water + lithium bromide + lithium nitrate + 1, 3-propanediol. *J. Chem. Eng. Data* **42**, 145–148 (1997)
19. De Lucas, A., Donate, M., Rodríguez, J.F.: vapor pressures, densities, and viscosities of the (water + lithium bromide + sodium formate) system and (water + lithium bromide + potassium formate) system. *J. Chem. Eng. Data* **48**, 18–22 (2003)
20. Donate, M., Rodríguez, L., De Lucas, A., Rodríguez, J.F.: Thermodynamic evaluation of new absorbent mixtures of lithium bromide and organic salts for absorption refrigeration machines. *Int. J. Refrig.* **29**, 30–35 (2006)
21. Jing, L., Zheng, D., Fan, L., Wu, X., Dong, L.: vapor pressure measurement of the ternary systems H₂O + LiBr + [Dmim]Cl, H₂O + LiBr + [Dmim]BF₄, H₂O + LiCl + [Dmim]Cl, and H₂O + LiCl + [Dmim]BF₄. *J. Chem. Eng. Data* **56**, 97–101 (2011)
22. Luo, C., Li, Y., Chen, K., Li, N., Su, Q.: Thermodynamic properties and corrosivity of a new absorption heat pump working pair: lithium nitrate + 1-butyl-3-methylimidazolium bromide + water. *Fluid Phase Equilib.* **451**, 25–39 (2017)
23. Tsai, C.Y., Soriano, A.N., Li, M.H.: Vapour pressures, densities, and viscosities of the aqueous solutions containing (triethylene glycol or propylene glycol) and (LiCl or LiBr). *J. Chem. Thermodyn.* **41**, 623–631 (2009)
24. Królikowska, M., Romańska, K.: The experimental study on the influence of crown ethers and glycols on the mutual solubility of lithium bromide in water. *Fluid Phase Equilib.* **483**, 175–181 (2019)
25. Królikowska, M., Zawadzki, M.: The experimental study on influence of zwitterionic compounds on solubility of lithium bromide in water. *Fluid Phase Equilib.* **475**, 18–24 (2018)
26. Kim, J.-S., Park, Y., Lee, H.: Densities and viscosities of the water + lithium bromide + ethanolamine system. *J. Chem. Eng. Data* **41**, 678–680 (1996)
27. De Lucas, A., Donate, M., Rodríguez, J.F.: Vapour pressures, densities, and viscosities of the (water + lithium bromide + potassium acetate) system and (water + lithium bromide + sodium lactate) system. *J. Chem. Thermodyn.* **38**, 123–129 (2006)
28. Park, Y., Kim, J.-S., Lee, H.: Thermodynamic properties of the lithium bromide + diethanolamine + water system. *ASHREA Trans.* **103**, 175–181 (1997)
29. Jing, L., Danxing, Z., Lihua, F., Xianghong, W., Li, D.: Vapor pressure measurement of the ternary systems H₂O + LiBr + [Dmim]Cl, H₂O + LiBr + [Dmim]BF₄, H₂O + LiCl + [Dmim]Cl, and H₂O + LiCl + [Dmim]BF₄. *J. Chem. Eng. Data* **56**, 97–101 (2011)
30. Sánchez, P.B., Traikia, M., Dequid, A., Pádua, A.A.H., García, J.: Molecular understanding of pyridinium ionic liquids as absorbents with water as refrigerant for use in heat pumps. *AIChE J.* **63**, 3523–3531 (2017)

31. Luo, C., Chen, K., Li, Y., Su, Q.: Crystallization temperature, vapor pressure, density, viscosity, and specific heat capacity of the $\text{LiNO}_3/[\text{BMIM}]\text{Cl}/\text{H}_2\text{O}$ ternary system. *J. Chem. Eng. Data* **62**, 3043–3052 (2017)
32. Zhang, X., Gao, N., Wu, Y., Chen, G.: Vapor pressure measurement for the ternary system of water, lithium bromide, and 1-ethyl-3-methylimidazolium acetate. *J. Chem. Eng. Data* **63**, 781–786 (2018)
33. Królikowska, M., Hofman, T.: The influence of bromide-based ionic liquids on solubility of LiBr (1) + water (2) system. Experimental (solid+ liquid) phase equilibrium data. Part 1. *J. Mol. Liq.* **273**, 606–614 (2019)
34. Królikowska, M., Zawadzki, M., Skonieczny, M.: The influence of bromide-based ionic liquids on solubility of LiBr (1) + water (2) system. Experimental (solid + liquid) phase equilibrium data. Part 2. *J. Mol. Liq.* **265**, 316–326 (2018)
35. Halayqa, M., Zawadzki, M., Domańska, U., Plichta, A.: Polymer–ionic liquid–pharmaceutical conjugates as drug delivery systems. *J. Mol. Struct.* **1180**, 573–584 (2019)
36. Królikowska, M., Zawadzki, M.: Transport properties and thermodynamic characterization of aqueous solutions of morpholinium-based ionic liquids. *J. Mol. Liq.* **251**, 358–368 (2018)
37. Klamt, A., Eckert, F.: COSMO-RS: a novel and efficient method for the a priori prediction of thermophysical data of liquids. *Fluid Phase Equilib.* **172**, 43–72 (2000)
38. Klamt, A.: COSMO-RS: From Quantum Chemistry to Fluid Phase Thermodynamics and Drug Design. Elsevier, Amsterdam, The Netherlands (2005)
39. Eckert, F., Klamt, A.: COSMOtherm (version 18.0.2, revision 4521). COSMOlogic GmbH & Co. KG, Leverkusen (2015)
40. Ahlrichs, R., Bär, M., Häser, M., Horn, H., Kölmel, C.: Electronic structure calculations on workstation computers: the program system turbomole. *Chem. Phys. Lett.* **162**, 165–169 (1989)
41. Perdew, J.P.: Density-functional approximation for the correlation energy of the inhomogeneous electron gas. *Phys. Rev. B Condens. Matter Mater. Phys.* **33**, 8822–8824 (1986)
42. Becke, A.D.: Density functional exchange energy approximation with current asymptotic behavior. *Phys. Rev. A At. Mol. Opt. Phys.* **38**, 3098–3100 (1988)
43. Schäfer, A., Huber, C., Ahlrichs, R.: Fully optimized contracted Gaussian basis sets of triple zeta valence quality for atoms Li to Kr. *J. Chem. Phys.* **100**, 5829–5835 (1994)
44. Klamt, A.: Conductor-like screening model for real solvents: a new approach to the quantitative calculation of solvation phenomena. *J. Phys. Chem.* **99**, 2224–2235 (1995)
45. Lannung, A.: Measurement of the vapor pressure of aqueous solutions of the alkali halogenides. *Z. Phys. Chem. A* **170**, 134–144 (1934)
46. Pennington, W.: How to find accurate vapor pressure of LiBr water solution. *Refriger. Eng.* **63**, 57–61 (1955)
47. Uemura, T., Hasaba, S.: Studies on the lithium bromide–water absorption refrigerating machine. *Tech. Rep. Kansai Univ.* **6**, 31–55 (1964)
48. Boryta, D.A., Maas, A.J., Grant, C.B.: Vapor pressure–temperature–concentration relation for system lithium bromide and water (40–70% lithium bromide). *J. Chem. Eng. Data* **20**, 316–319 (1975)
49. Sada, E., Morisue, T., Miyahara, K.: Salt effects on vapor–liquid equilibrium of isopropanol–water system. *J. Chem. Eng. Jpn.* **8**, 196–201 (1975)
50. Matsuda, A., Munakata, T., Yoshimaru, T., Kubara, T., Fuchi, H.: Measurement of vapor pressures of lithium bromide–water solutions. *Kagaku Kogaku Ronbunshu* **6**(2), 119–122 (1980)
51. Iyoki, S., Uemura, T.: Vapor pressure of the water–lithium bromide system and the water–lithium bromide–zinc bromide–lithium chloride system at high temperatures. *Int. J. Refriger.* **12**, 278–282 (1989)
52. Patil, K.R., Tripathi, A.D., Pathak, G., Katti, S.S.: Thermodynamic properties of aqueous electrolyte solutions. 1. Vapor pressure of aqueous solutions of LiCl, LiBr, and LiI. *J. Chem. Eng. Data* **35**, 166–168 (1990)
53. Lenard, J.L.Y., Jeter, A.M., Teja, A.S.: Properties of lithium bromide–water solutions at high temperatures and concentrations, Part IV: Vapor pressure. *ASHRAE Trans.* **98**, 167–172 (1992)
54. Pátek, J., Klomfar, J.: A computationally effective formulation of the thermodynamic properties of LiBr–H₂O solutions from 273 to 500 K over full composition range. *Int. J. Refriger.* **29**, 566–578 (2006)
55. Wimby, J.M., Berntsson, T.S.: Viscosity and density of aqueous-solutions of LiBr, LiCl, ZnBr₂, CaCl₂, and LiNO₃. 1. Single salt-solutions. *J. Chem. Eng. Data* **39**, 68–72 (1994)
56. Stankus, S.V., Khairulin, R.A., Gruzdev, V.A., Verba, O.I.: The density of aqueous solutions of lithium bromide at high temperatures and concentrations. *High Temp. (Engl. transl.)* **45**, 429–431 (2007)
57. Reiser, S., Horsch, M., Hasse, H.: Temperature dependence of the density of aqueous alkali halide salt solutions by experiment and molecular simulation. *J. Chem. Eng. Data* **59**, 3434–3448 (2014)

58. Desnoyers, J.E., Perron, G.: The viscosity of aqueous solutions of alkali and tetraalkylammonium halides at 25 °C. *J. Solution Chem.* **1**, 199–212 (1972)
59. Shekaari, H., Zafarani-Moattar, M.T., Golmohammadi, B.: Thermodynamic and transport properties of ionic liquids, 1-alkyl-3-methylimidazolium thiocyanate in the aqueous lithium halides solutions. *J. Chem. Thermodyn.* **141**, 105953 (2020)

Publisher's Note Springer Nature remains neutral with regard to jurisdictional claims in published maps and institutional affiliations.